Supporting Information for

On-Chip Construction of Liver Lobule-like Microtissue and Its Application for Adverse Drug Reaction Assay

*Chao Ma, Lei Zhao, En-Min Zhou, Juan Xu, Shaofei Shen, and Jinyi Wang**

Colleges of Veterinary Medicine and Science, Northwest A&F University, Yangling, Shaanxi 712100, P. R. China.

* Phone: + 86-29-870 825 20. Fax: + 86-29-870 825 20. E-mail: jywang@nwsuaf.edu.cn.

Abstract. This Supporting Information includes all additional information as noted in the manuscript.

Supplementary Materials and Methods

Materials and reagents. RTV 615 polydimethylsiloxane (PDMS) prepolymer and curing agent were purchased from Momentive Performance Materials (Waterford, NY, USA). The surface-oxidized silicon wafers were obtained from Shanghai Xiangjing Electronic Technology Ltd. (Shanghai, China). The AZ 50XT photoresist and developer were bought from AZ Electronic Materials (Somerville, NJ, USA). The SU-8 2025 photoresist and developer were purchased from Microchem (Newton, MA, USA). Rat Collagen-I high concentration was bought from BD Company (Franklin Lakes, NJ, USA). Resorufin, 4-methylumbelliferone (4-MU), fluorescein diacetate (FDA), propidium iodide (PI), and 3-(4,5-dimethylthiazol-2-yl)-2,5-diphenyltetrazolium bromide (MTT) were bought from Sigma-Aldrich (St. Louis, MO, USA). Dulbecco's Modified Eagle Medium (DMEM), fetal bovine serum (FBS), CellTracker Green CMFDA, CellTracker orange CMRA, and trypsin were obtained from Gibco/Life Technologies (New York, NY, USA). 7-ethoxyresorufin (7-ER) was obtained from AnaSpec, Inc. (Fremont, CA, USA). All solvents and other chemicals were purchased from local commercial suppliers and were of analytical reagent grade, unless otherwise stated. All aqueous solutions were prepared using ultra-purified water supplied by a Milli-Q system (Millipore®).

Cell culture. A human liver cell line HepG2 and an immortalized human aortic endothelial cell line HAEC were obtained from the Chinese Academy of Sciences (Shanghai, China). The cells were cultured using DMEM supplemented with 10% FBS, 100 U/mL penicillin, and 100 μg/mL streptomycin in a humidified atmosphere of 5% CO_2 at 37 °C, except that the culture medium for HAECs contained 100 μg/mL heparin. The cells were normally passaged at a ratio of 1:3 every three days to maintain them in the exponential growth phase. When the cells reached confluence, they were harvested through trypsinization with 0.25% trypsin in Ca^{2+}- and Mg^{2+}-free Hank's balanced salt solution (CMF-HBSS) at 37 °C before use. Trypsinization was stopped by adding freshly supplemented DMEM. The cell suspension was centrifuged at 1000 rpm for 5 min. The cells were then resuspended in DMEM or neutralized collagen solution for further use. In addition, to clearly distinguish the coexistence of HepG2

cells and HAECs, the two types of cells were pre-stained with CellTracker Green CMFDA and CellTracker Orange CMRA (10 μmol/L in DMEM, 45 min), respectively, following a wash step with phosphate-buffered saline (PBS, 0.01 M, pH 7.4), prior to be loaded into the device for the subsequent studies.[S1]

Device design and fabrication. As shown in Figure S1, the biomimetic microfluidic device utilized in the current study was designed using software AutoCAD (Autodesk, Inc., San Rafael, CA, USA), with inspiration from the natural architecture of liver and previous report.[S2] The device consisted of four layers: a fluidic layer, a control layer, a thin PDMS layer, and a glass slide (Figure S1b and S1c). The fluidic layer had a hexagonal cell culture chamber with three sets of pillar arrays, i.e., trapezoid pillar arrays (labelled with green), a cylindrical pillar array (magenta) and a quadrangular pillar array (cyan) (Figure S1a). The trapezoid pillar arrays were made up of 24 pillar arrays (consisted of 50 μm-isosceles trapezoid) that were 1180 μm (length) × 140 μm (width) × 40 μm (height) and 24 pillar arrays (consisted of 20 μm-isosceles trapezoid) that were 360 μm (length) × 65 μm (width) × 40 μm (height). These micro-engineered pillar arrays were used here, in particular, to immobilize and support the collagen hydrogel-encapsulated cells [in the current study we called them cells in gel in pillar array (CiGiPA)], as well as to retain the 3D cell–cell and cell–matrix interactions. The cylindrical pillar array (consisted of cylinders with the diameter of 100 μm) was set to prevent microchamber from common subsidence. The square pillar array (consisted of squares with side length of 50 μm) was set to mimic the lobule interval situated between neighboured liver lobule. In the control layer, there was a pneumatic microvalve system composed of two independently actuated valves (i.e., the inner and outer valve), which could be dynamically operated to aid the cell loading operation. The thin PDMS layer was used as an adhesive/supporting layer to assemble the control layer onto the glass slide and enable the valves to withstand high actuation pressure after irreversibly bonding with the control layer. One inlet and six outlets were used for cell loading, nutrient supply, chamber purging, and waste exclusion. During the cultivation period, cell culture medium was slowly and continuously perfused into the microfluidic chamber through the inlet with a medium reservoir and removed from the outlets twice daily.

The device was fabricated with a multilayer soft lithography method, as depicted in Figure S2.[S3-5] In brief, to prepare the mold utilized for fabricating the fluidic components, a 40-μm thick positive photoresist (AZ 50XT) was spin-coated onto a silicon wafer. After ultraviolet (UV) light exposure, the fluidic components on the wafer were developed using an AZ 400K developer. The mold for the control channels was made by introducing a 25-μm thick negative photoresist (SU8-2025) pattern on a silicon wafer. Before fabricating the microfluidic device, both the fluidic and control molds were exposed to trimethylchlorosilane vapor for 3 min. A well-mixed PDMS pre-polymer (RTV 615 A and B in a 10 to 1 ratio, w/w) was poured onto the fluidic mold, which was placed in a Petri dish to yield a 5 mm thick fluidic layer. The PDMS pre-polymer (RTV 615 A and B in a 20 to 1 ratio, w/w) was also spin-coated onto the control mold (2,000 rpm, 60 s, ramp 15 s) to obtain the thin control layer. The thick fluidic layer and thin control layer were cured in an 80 °C oven for 90 min and 20 min, respectively. After incubation, the thick fluidic layer was peeled off the mold, and holes were introduced into the fluidic layer for reagent and cell sample supply access as well as waste exclusion. The fluidic layer was then trimmed, cleaned, and aligned onto the thin control layer. After baking at 80 °C for 48 h, the assembled layers were peeled off the control mold, and another set of holes was punched for access to control channels. These assembled layers were then placed on top of a glass slide (2,000 rpm, 30 s, ramp 15 s) coated with the PDMS pre-polymer (RTV 615 A and B in a 10 to 1 ratio, w/w) that had been cured for 8 min in the oven (80 °C). The microfluidic device was ready for use after baking at 80 °C for 72 h.

CYP-1A1/2 activity assay. CYP-1A1/2 activity was assessed by measuring O-dealkylation of the substrate 7-ethoxyresorufin (7-ER) to form the fluorescent product resorufin.[S6] Briefly, after 72-h culture, cells were washed twice with PBS, and then incubated with 400 μL PBS containing 2.5 μM 7-ER, along with 10 μM dicumarol to prevent subsequent metabolism of resorufin. After the incubation was continued for 1 h, the supernatants were collected and pipetted into 96-well plates. The fluorescence intensities of samples were determined at 531/595 nm (ex/em) using Wallac 1420 VICTOR^{X5} multilabel plate readers (Perkin-Elmer, Waltham, MA, USA). The concentration of produced resorufin was determined based on a standard curve generated in PBS spiked with 0, 2.5, 5,

10, 25, 50, 100, 250, 500 and 1000 nM. All the data were normalized to the seeded HepG2 cells, and the activity was expressed as pmol of resorufin formed per hour and per million HepG2 cells (pmol/million cells/h). For enzyme induction and inhibition experiments, culture models were pretreated with a known pharmacological inducer [i.e., 50 μM omeprazole (OME)] or inhibitor [i.e., 25 μM ciprofloxacin (CPFX)] of CYP-1A1/2 for 48 h after 24-h post-establishment.[S7-9] Vehicle controls were pre-treated with corresponding concentrations of dimethyl sulfoxide (DMSO). The media were changed every 12 h during the treatment. Stock solutions of 7-ER and OME were prepared in DMSO at a concentration of 2.5 mM and 50 mM, respectively. Stock solution of CPFX was prepared in 0.1 N HCl at 10 mM. Solutions of these compounds were prepared and stored in dark, and the reaction was performed in a room with dim lighting.

UGT activity assay. UGT activity was determined by quantification of the substrate 4-methylumbelliferone (4-MU) transferred into 4-methylumbelliferyl glucuronide (4-MUG) before and after cells were incubated with the substrate.[S2] Briefly, after 72-h culture, cells were washed twice with PBS, followed by incubation with 400 μL PBS containing 100 μM 4-MU for 4 h. And then the cell supernatants were collected and pipetted into 96-well plates. The fluorescence intensities of samples were determined at 355/460 nm (ex/em) using the multilabel plate readers. The remaining 4-MU concentration was determined based on a standard curve generated in PBS spiked with 0, 1.5, 3, 6, 12.5, 25, 50 and 100 μM. All the data were normalized to the seeded HepG2 cells, and the activity was expressed as nmol of 4-MUG produced per hour and per million HepG2 cells (nmol/million cells/h). For enzyme induction and inhibition experiments, culture models were pre-treated with an inducer [i.e., 50 μM rifampicin (RIF)] or inhibitor [i.e., 200 μM probenecid (PBD)] of UGT enzymes for 48 h after 24-h post-establishment.[S2,S9] Vehicle controls were pre-treated with corresponding concentrations of DMSO. The media were changed every 12 h during the treatment. Stock solutions of RIF and PBD were prepared in DMSO at a concentration of 50 mM and 200 mM, respectively. Solutions of these compounds were prepared and stored in dark, and the reaction was performed in a room with dim lighting.

Drug concentration determination. To determine working doses used for drug sensitivity assessment, dose-response profiles of the chosen model drugs were established using conventional MTT assay. The MTT assay quantified the activity of mitochondrial dehydrogenase enzymes in cells, which cleaved the substrate tetrazolium ring to form a purple precipitate formazan.[S4] Generally, HepG2 cells were seeded in 96-well plates (1×10^4 cells/well, 100 μL medium; NUNC, USA), and cultured at 37 °C in a humidified 5% CO_2 atmosphere for 24 h. Drugs were added to FBS-free DMEM at various concentrations (i.e., 0.1, 0.2, 0.5, 1, 10, 20, 40, 60, 80 or 100 mM for APAP; 0.5, 1, 2, 5, 10, 20, 40, 80 or 100 mM for INH; 50, 100, 200, 300, 500, 1000, 1500, 1750, 2000 or 2500 μM for RIF) and incubated with cells for 24 h. Subsequently, the culture medium was replaced with 100 μL PBS containing 10% (v/v) of the MTT solution (5 mg/mL in PBS), and the cells were cultured for an additional 4 h. The supernatant was discarded, and 100 μL dimethyl sulfoxide was added to dissolve the purple precipitate with the plates being placed on a shaker for 10 min. The reduction of MTT was quantified by photometrically recording the absorbance value (A) of each well at a wavelength of 490 nm using a microplate reader (Model 680, BIO-RAD, CA, USA). Each test was repeated at least three times with five replicates. Corresponding non-treated groups were run simultaneously during each experiment. Stock solutions of acetaminophen and isoniazid were, respectively, prepared in DMEM at 100 mM. The cell viability was calculated as follows

$$\text{Cell viability (\%)} = (A_d/A_c) \times 100\% \qquad (1)$$

where A_d and A_c are the absorbance values of the drug-treated and corresponding non-treated groups, respectively. The dose-response profiles were fitted in Origin 8.0 (Originlab Corp., Northampton, MA, USA). Three drug concentrations that induced low (~10%), middle (~30%), and high (~50%) hepatotoxicity were intentionally and respectively chosen for each drug, according to the dose-response profiles (Figure S13).

Supplementary Figure S1.

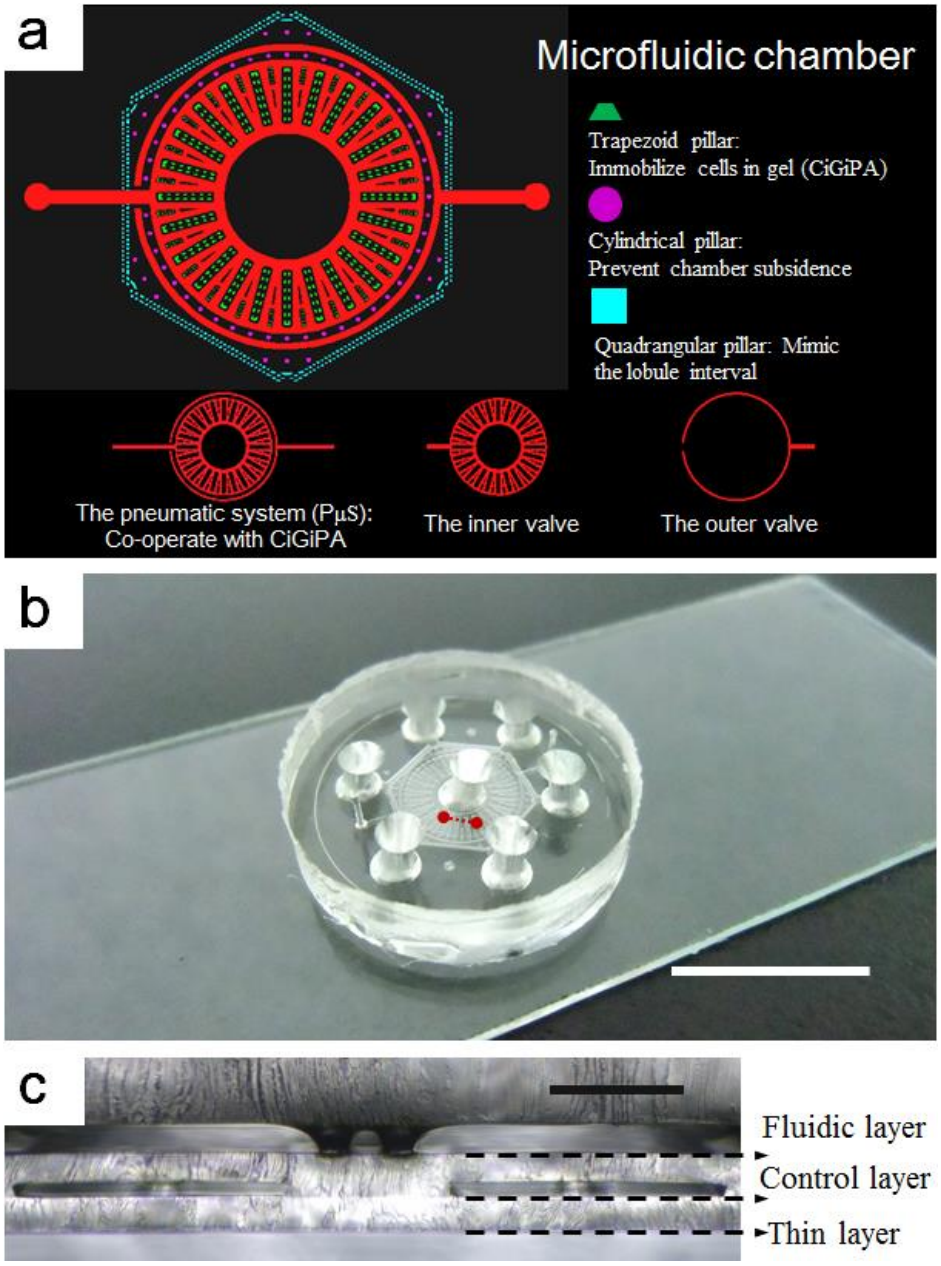

Figure S1. The microfluidic device. (a) Design of the biomimetic microfluidic device. In the fluidic layer, a hexagonal chamber with three sets of pillar arrays was engineered (labelled with different colors, i.e., green, magenta and cyan). In the control layer, a pneumatic system (PμS, labelled with red) was introduced, which was composed of two independent pneumatically actuated valves (i.e., inner valve and outer valve). (b) Optical image of the actual device. (c) Side-view of the device, corresponding to the red dot line in (b). The three PDMS layers were detached from the glass slide, and cut to produce a cross-section. Scale bar, (b) 1 cm, (c) 200 μm.

Supplementary Figure S2.

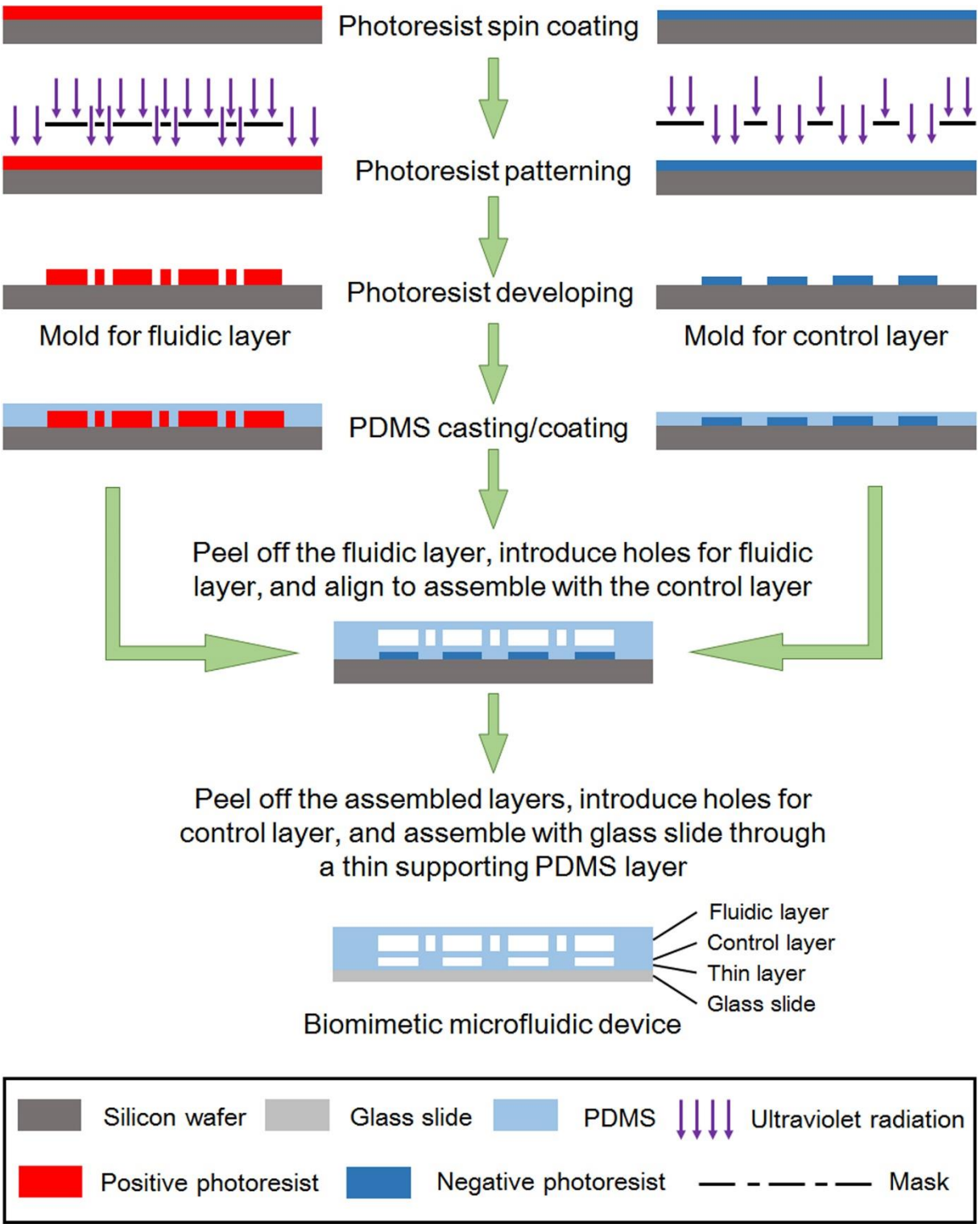

Figure S2. Multilayer soft lithography method for the fabrication of the biomimetic microfluidic device.

Supplementary Figure S3.

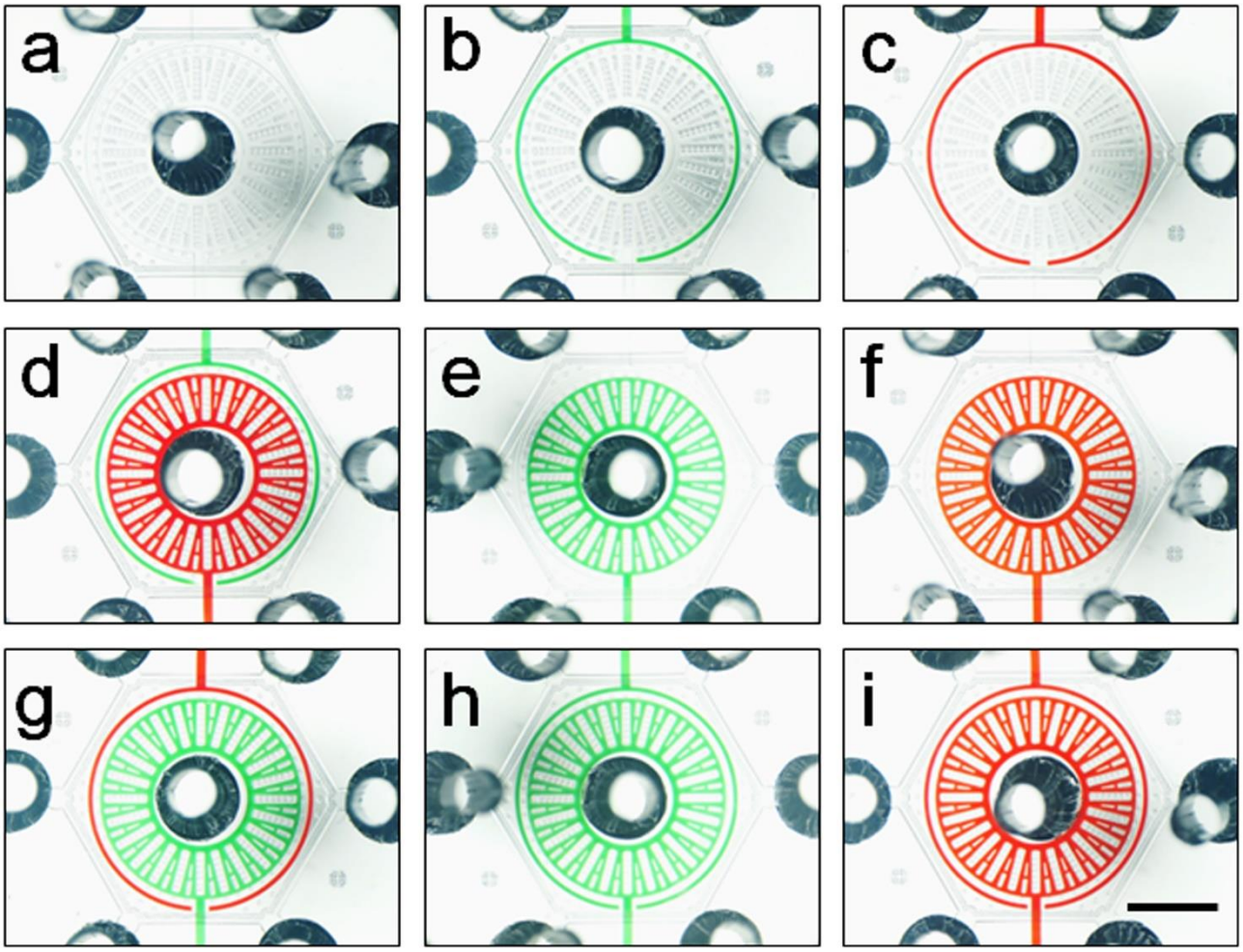

Figure S3. Display of the two well-designed valves in the pneumatic microvalve system (PμS) (a) Bright-field image of the microfluidic device. (b) and (c) The outer valve was colored by being filled with green or red food dye. (e) and (f) The inner valve was colored by being filled with green or red dye. (d) and (g) The valves were colored differently by being filled with the green or red dye, respectively. (h) and (i) The valves were colored by being filled with the same dye (green or red). Scale bar, 2 mm.

Supplementary Figure S4.

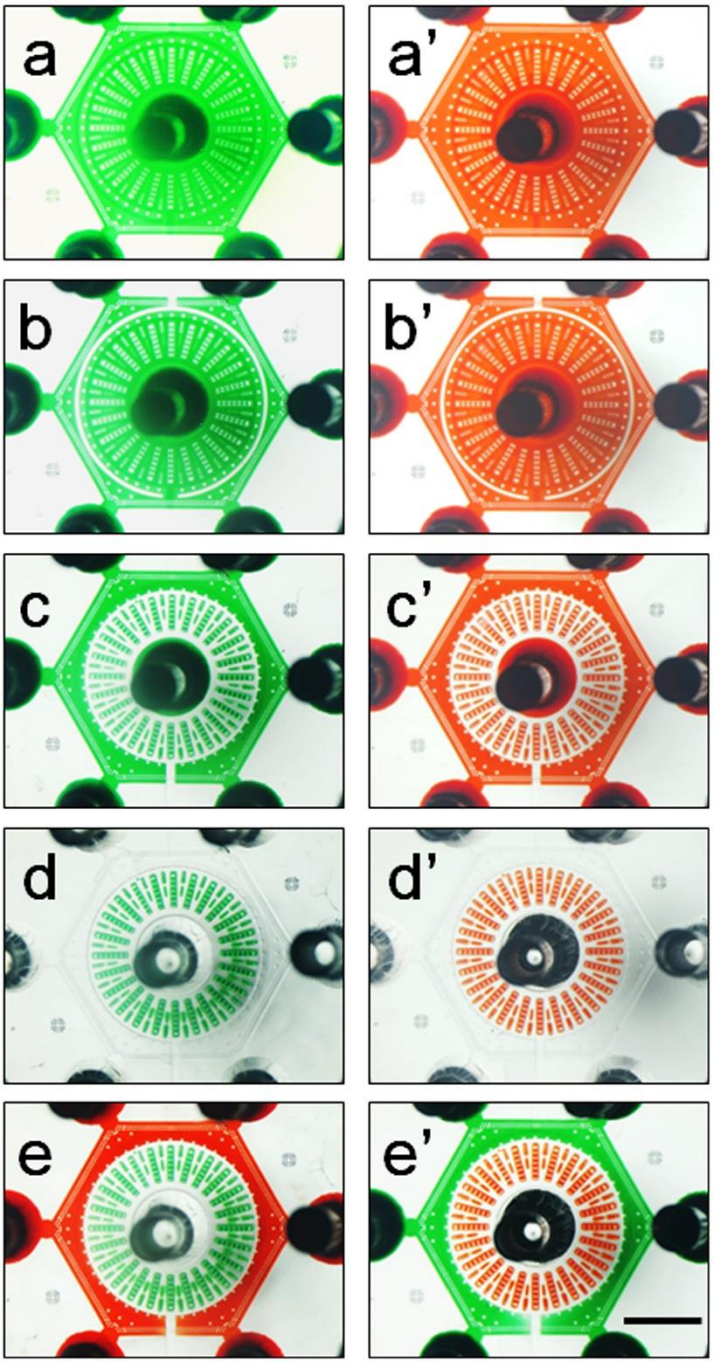

Figure S4. Working status of the PμS in the control layer. (a) and (a') The microfluidic chamber was filled with food dyes (green or red). (b) and (b') The actuation of the outer valve. (c) and (c') The actuation of the inner valve. (d) and (d') The restriction of a food dye in pillar arrays. (e) and (e') when the inner valve was actuated, a second food dye was loaded, which clearly demonstrated the microfluidic chamber. Scale bar, 2 mm.

Supplementary Figure S5.

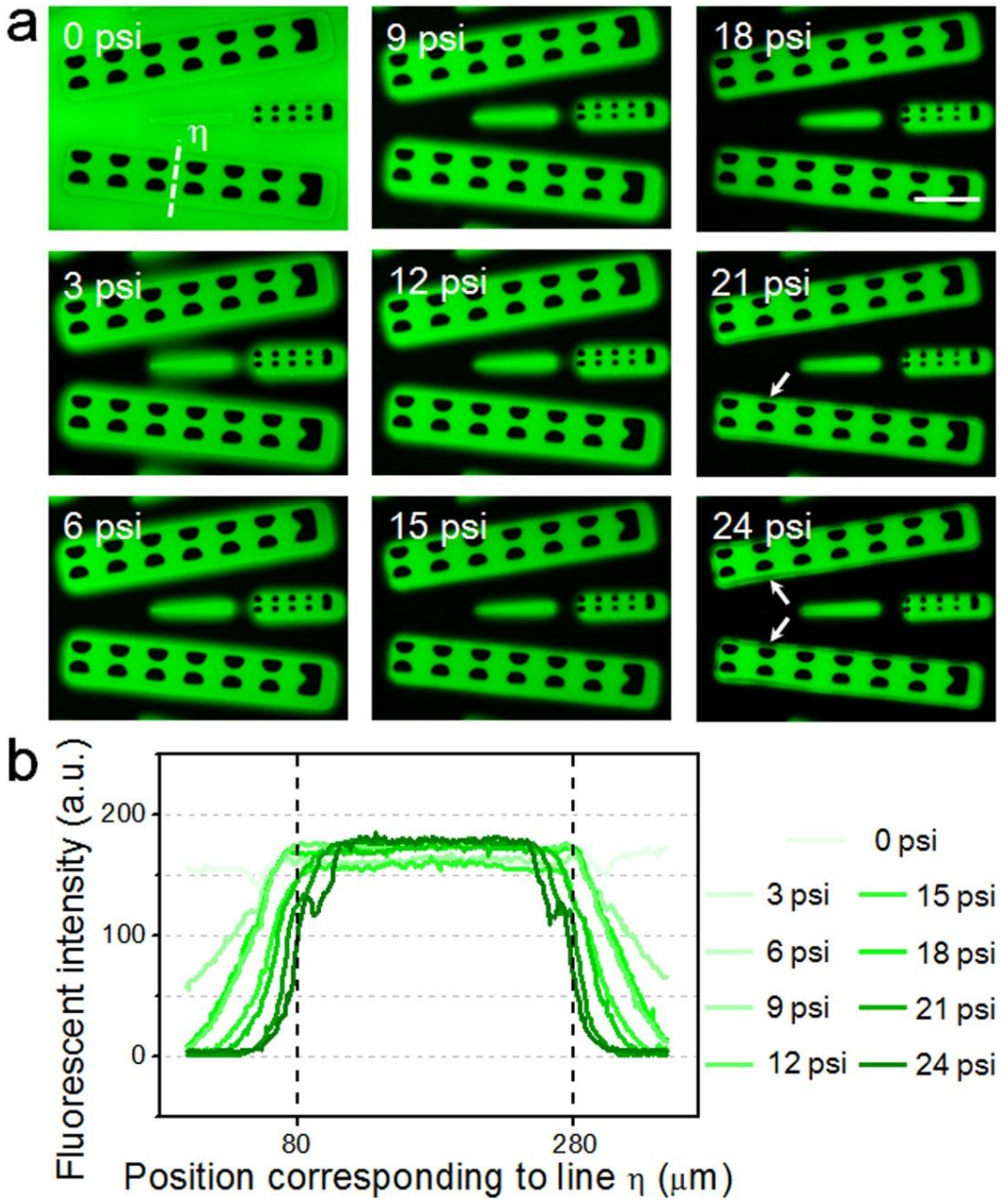

Figure S5. Working pressure for the inner valve. (a) The microfluidic chamber was fully filled with fluorescein solution (1 mM dissolved in $NaHCO_3$ solution). A serial of gas pressures were applied to actuate the inner valve. The deflection of inner valve indicated by the intensity of fluorescein was monitored. As shown in the images (white arrows), deformation of the pillar arrays occurred when the gas pressure was higher than 18 psi (i.e., 21 and 24 psi). (b) The fluorescent intensity at the line η was quantitatively measured. The result showed that a gas pressure of 18 psi was adequate to separate cord-like structures individually and define a hepatic cord network. Scale bar, 400 μm.

Supplementary Figure S6.

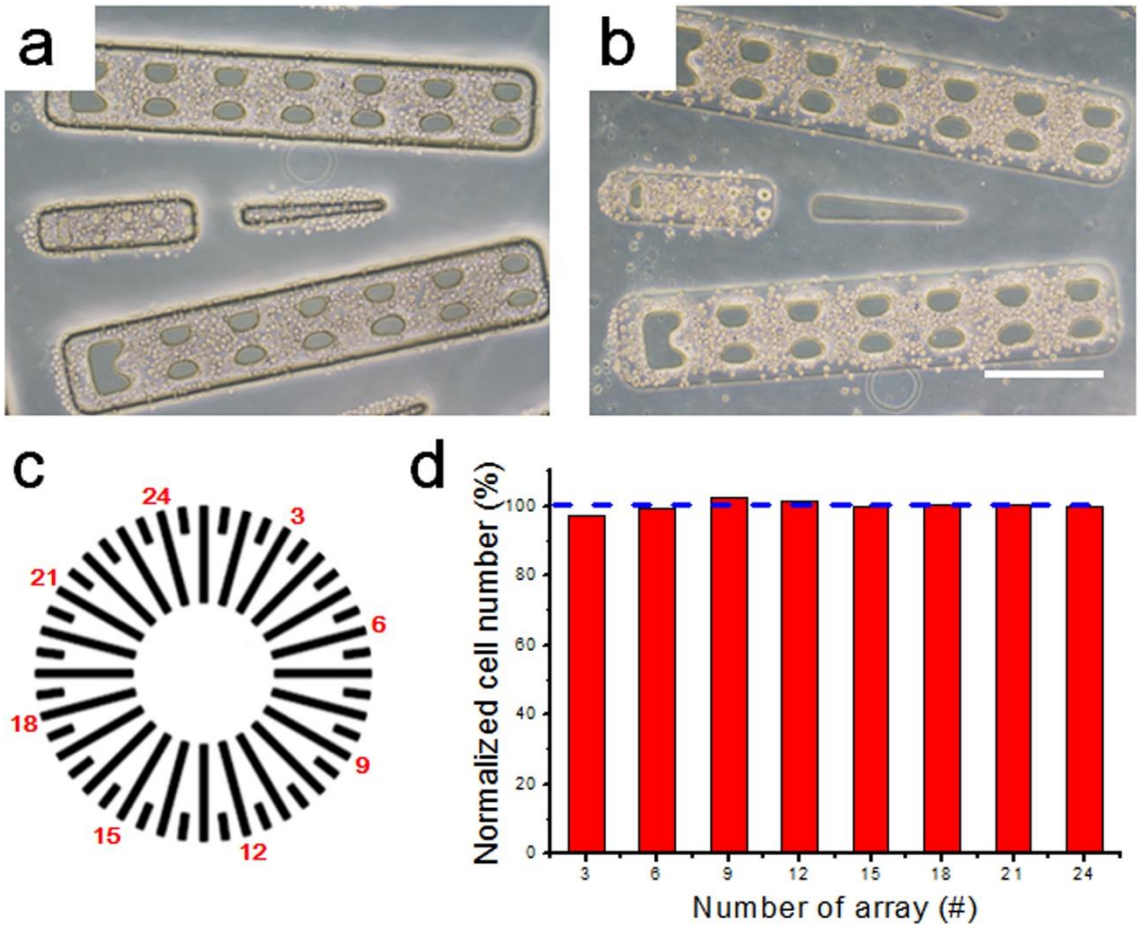

Figure S6. Immobilization of HepG2 cells in the microfluidic device. (a) HepG2 cells were immobilized in gel in pillar with the actuation of the inner valve. (b) After the deactuation of the inner valve, the hydrogel matrix located at the area without pillar arrays was easily washed away, indicating that the pillar array provided sufficient mechanical support. (c) The arrangement of the pillar array. (d) The number of HepG2 cells in every array, corresponding to (c), was manually quantified. The result showed that HepG2 cells were evenly distributed in every array. Scale bar, 300 μm.

Supplementary Figure S7.

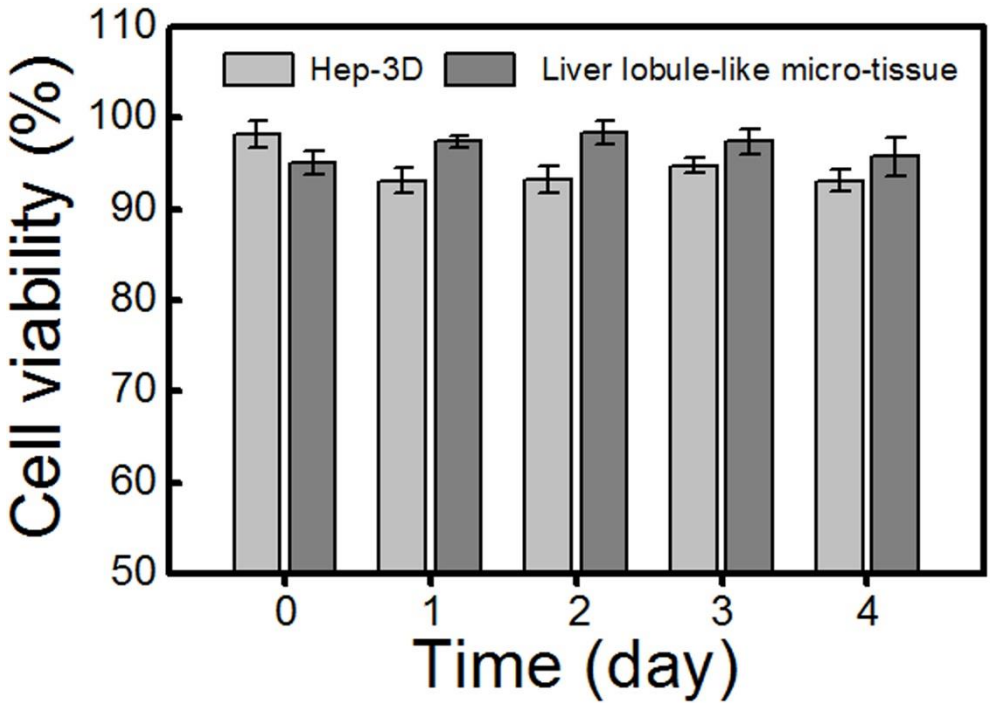

Figure S7. Quantitative data of the viability of HepG2 cells in Hep-3D and liver lobule-like micro-tissue culture models during 4-day culture, corresponding to Figure S9 and S11. The results showed that HepG2 cells in these two culture models had a great viability. Data are given as means ± SD, collected from three independent experiments.

Supplementary Figure S8.

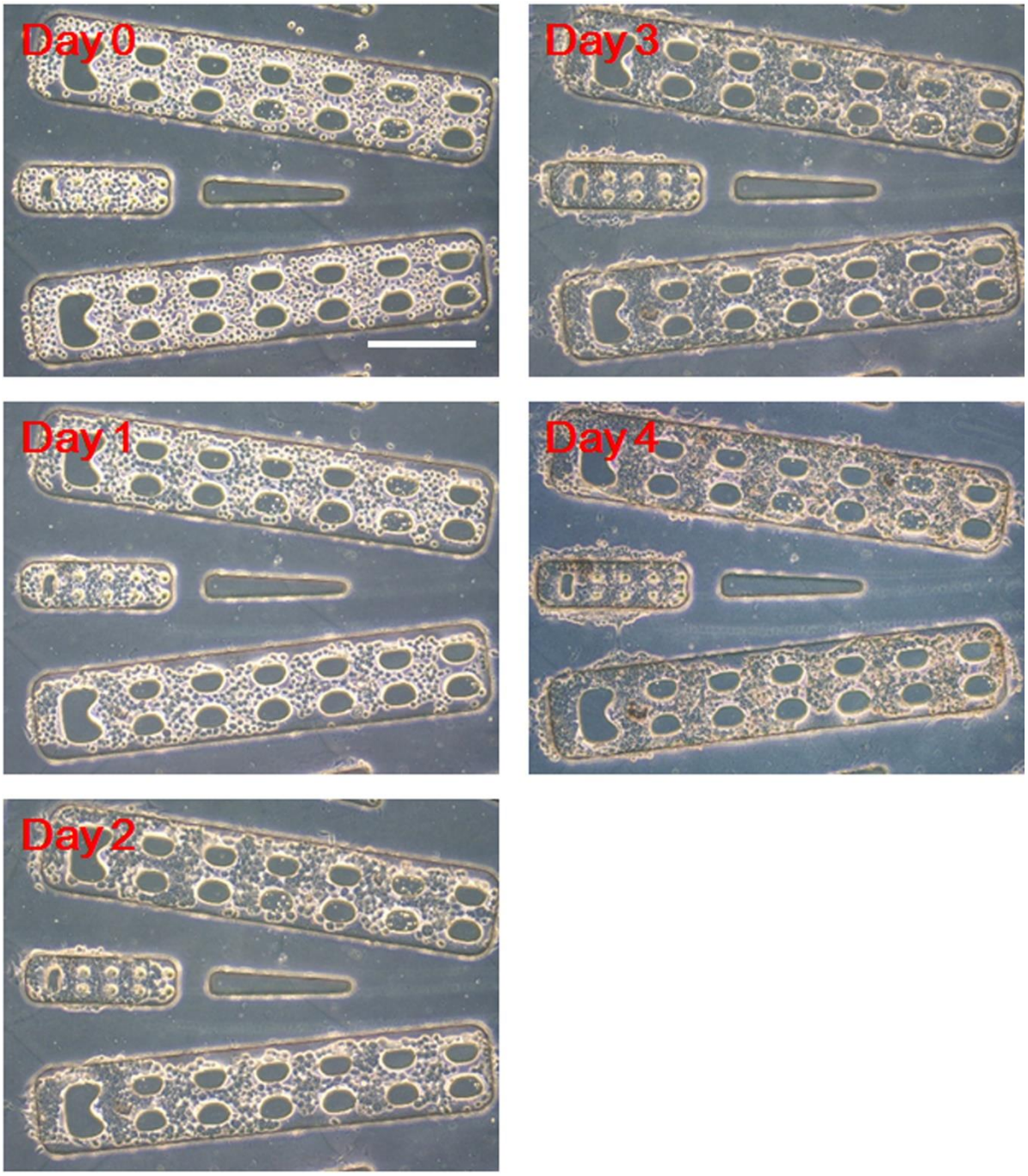

Figure S8. Time-lapse bright-field images of HepG2 cells in Hep-3D culture model at different time points in the microfluidic device. The images showed that during the 4-day culture period, HepG2 cells aggregated, proliferated and densified to form cord-like structures. Scale bar, 300 μm.

Supplementary Figure S9.

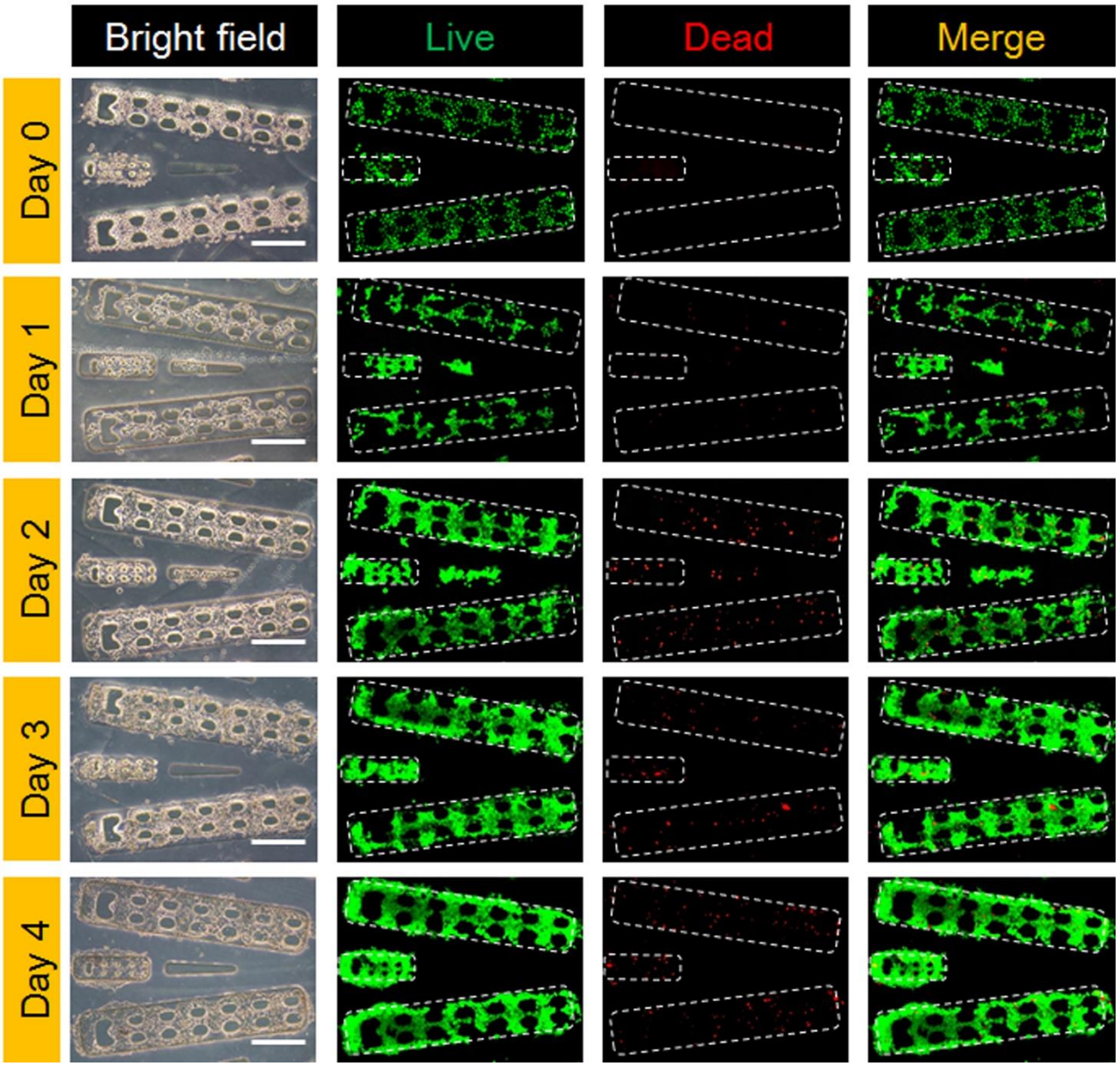

Figure S9. A set of bright-field images (the first column) and the corresponding FDA/PI co-staining fluorescent images (from the second to the fourth column: live, dead and merge) of HepG2 cells in Hep-3D culture model over the 4-day culture period. Live cells were stained green, and dead cells were stained red. Quantitative data of the viability of HepG2 cells was given in Figure S7. HepG2 cells showed high viability during the culture period. Scale bar, 300 μm.

Supplementary Figure S10.

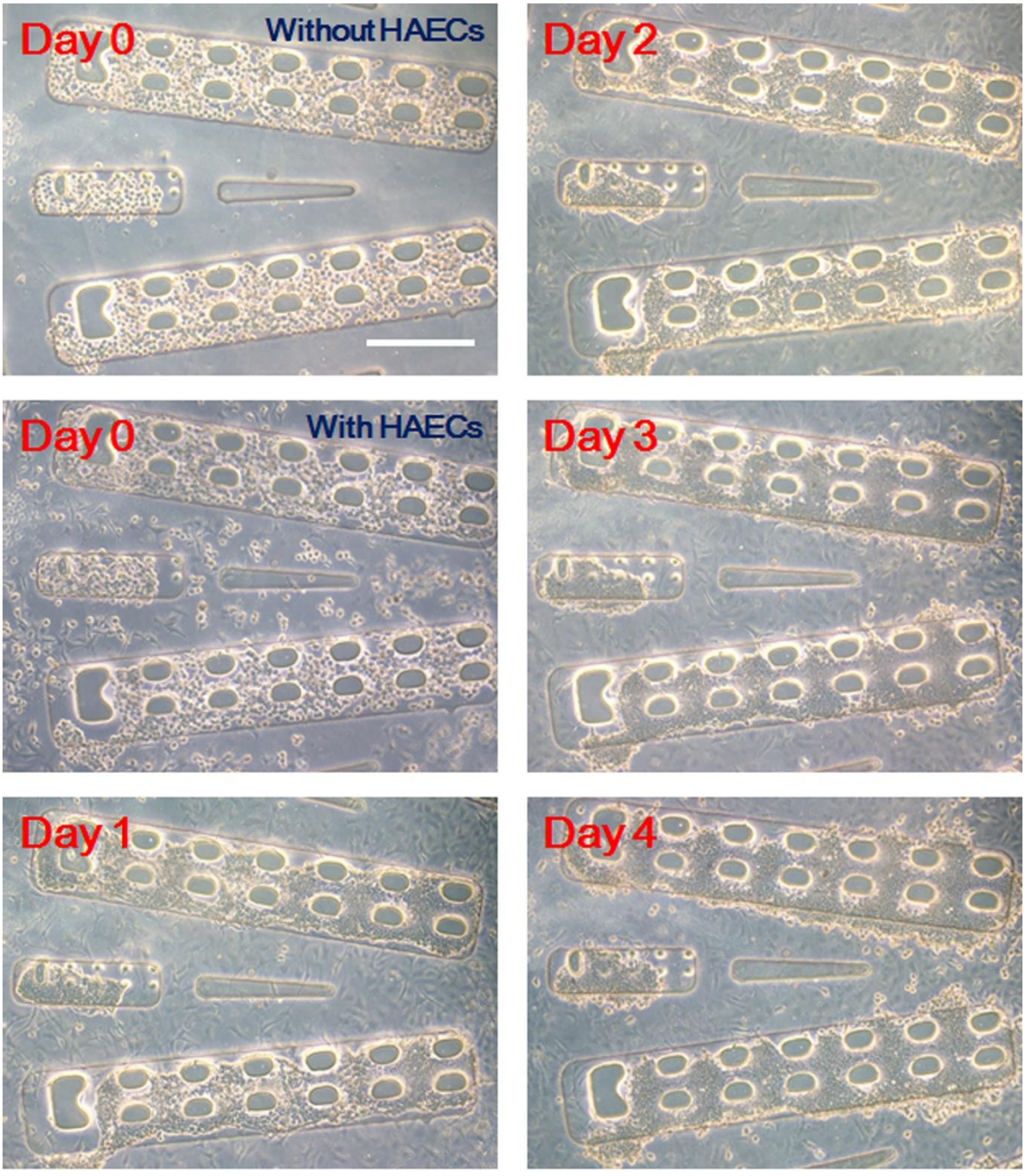

Figure S10. Time-lapse bright-field images of the liver lobule-like micro-tissue over the 4-day culture period in the microfluidic device. The images showed that HAECs spread and formed hepatic sinusoid-like structures, and meanwhile HepG2 cells aggregated, proliferated and densified to form cord-like structures. Scale bar, 300 μm.

Supplementary Figure S11.

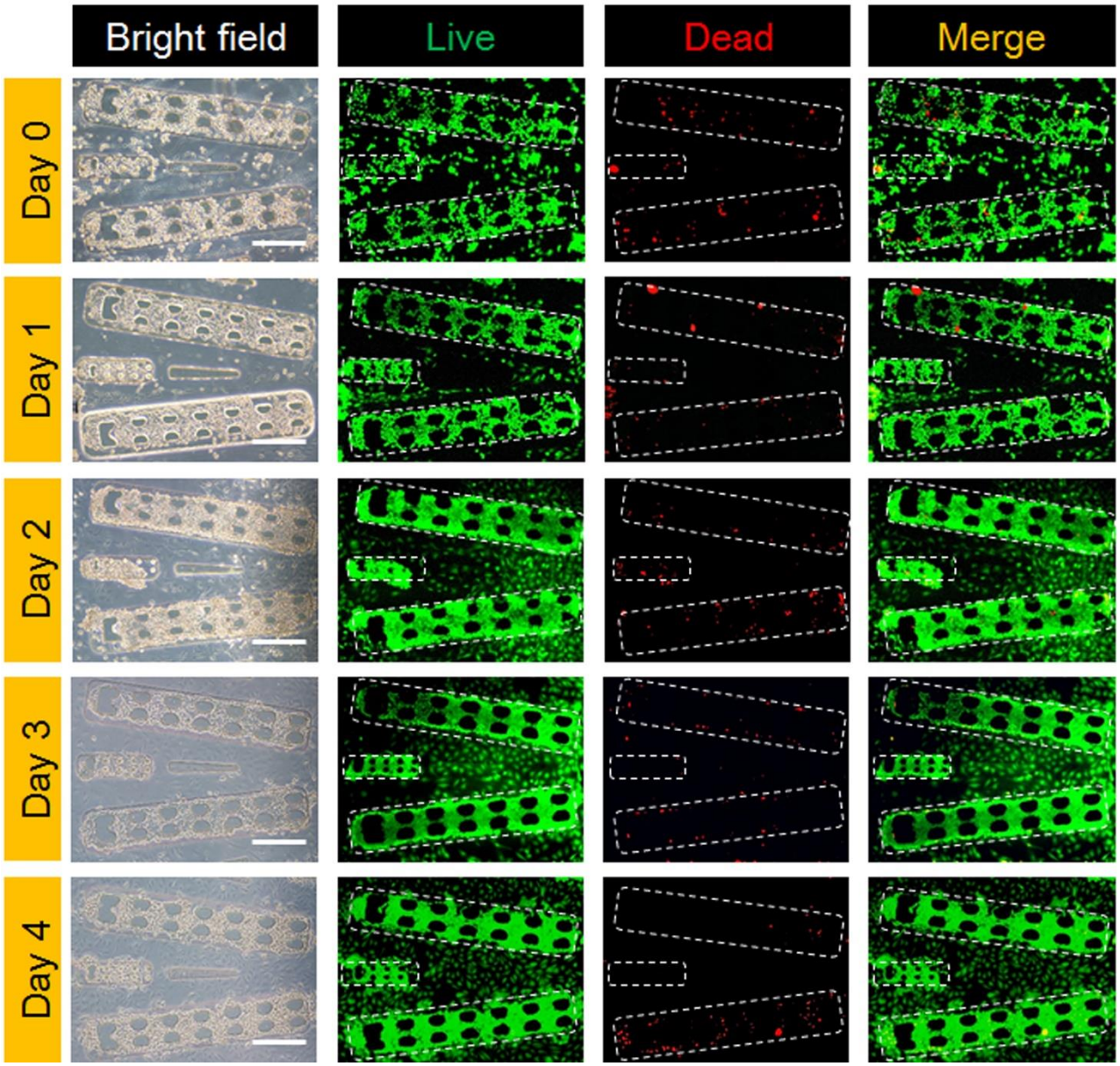

Figure S11. A set of bright-field images (the first column) and the corresponding FDA/PI co-staining fluorescent images (from the second to the fourth column: live, dead and merge) of the liver lobule-like micro-tissue during 4-day culture. Live cells were stained green, and dead cells were stained red. Quantitative data of the viability of HepG2 cells was given in Figure S7. Both HepG2 cells and HAECs showed high viability during the culture period. Scale bar, 300 μm.

Supplementary Figure S12.

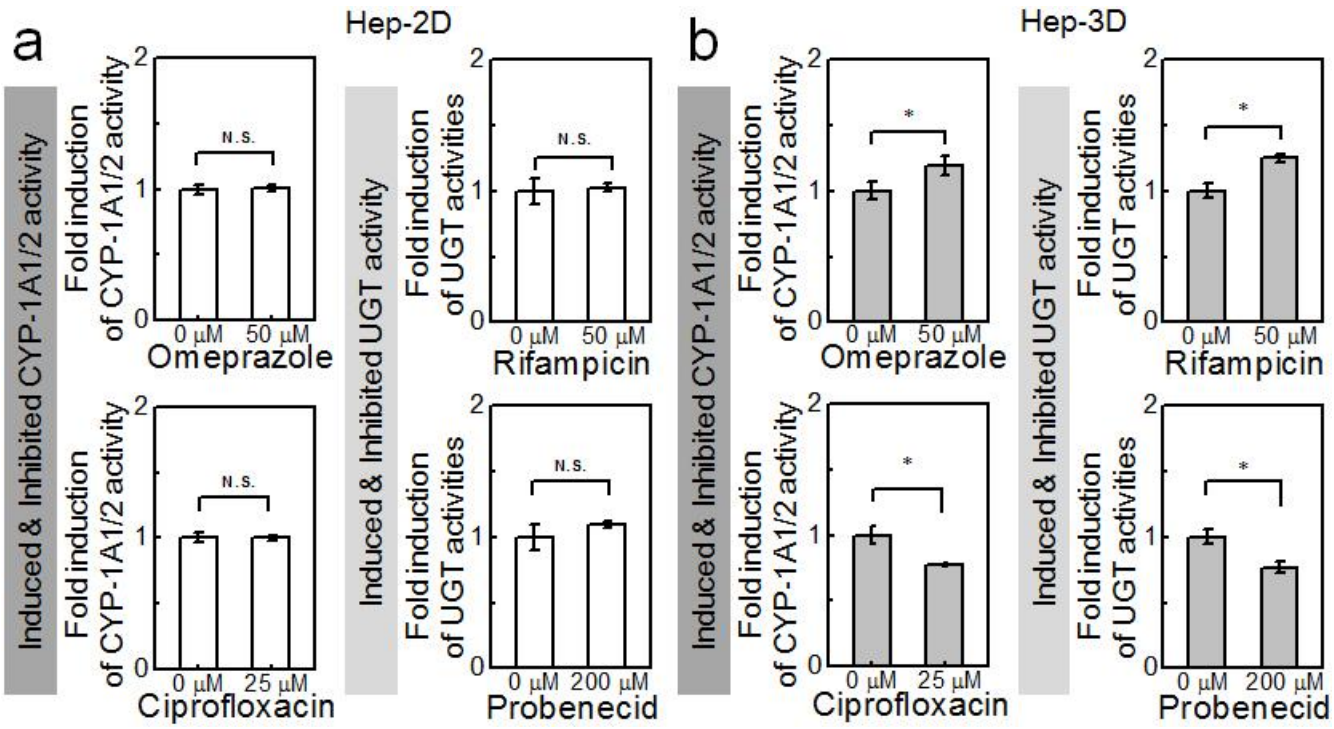

Figure S12. Hepatic enzyme activity of Hep-2D and Hep-3D culture models. (a) The enzyme activity of the Hep-2D culture model. The results showed that HepG2 cells cultured in 2D monolayer were not responsive to enzyme induction/inhibition. (b) The enzyme activity of the Hep-3D culture model. The results showed that HepG2 cells cultured in 3D were slightly responsive to enzyme induction/inhibition, indicating that the 3D microenvironment might be helpful to enable and/or improve the sensitivity of HepG2 cells to pharmacological inducers/inhibitors. Data are given as means ± SD, collected from three independent experiments. *: $P < 0.05$.

Supplementary Figure S13.

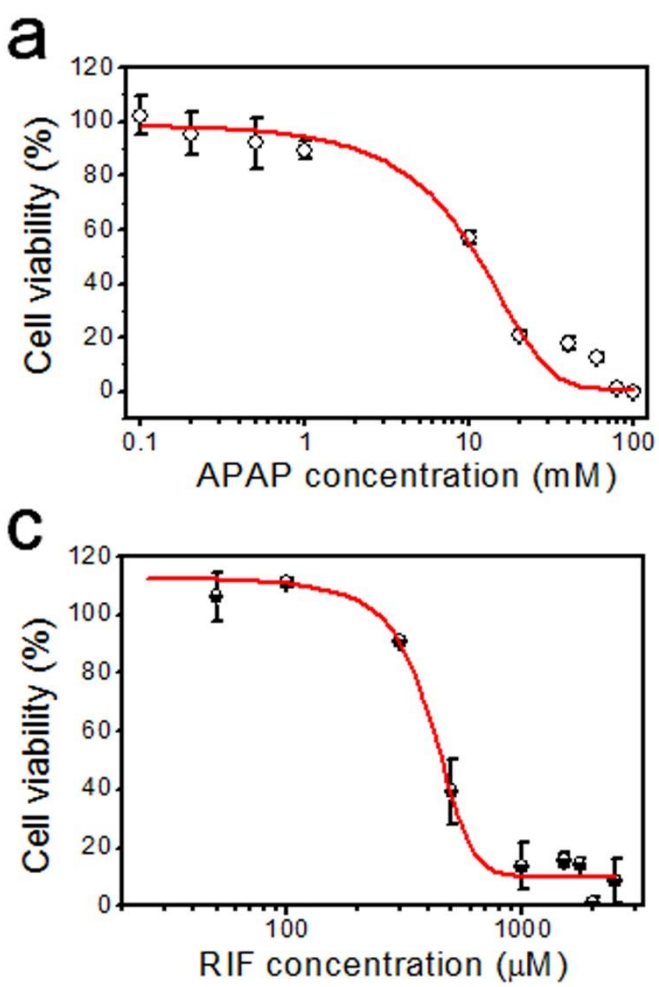

d

Drugs	Test concentrations (mM)		
APAP	5	10	20
INH	5	20	30
RIF	0.4	0.7	1

Figure S13. Acute hepatotoxicity profiles of three model drugs assessed by MTT assay. (a) Hepatotoxicity profile of acetaminophen (APAP). (b) Hepatotoxicity profile of isoniazid (INH). (c) Hepatotoxicity profile of rifampicin (RIF). (d) Drug concentrations chosen for drug sensitivity test. Three drug concentrations that induced low (~10%), middle (~30%), and high (~50%) hepatotoxicity were chosen for each drug, according to the dose-response profiles. Data are given as means ± SD, collected from three independent experiments.

Supplementary Figure S14.

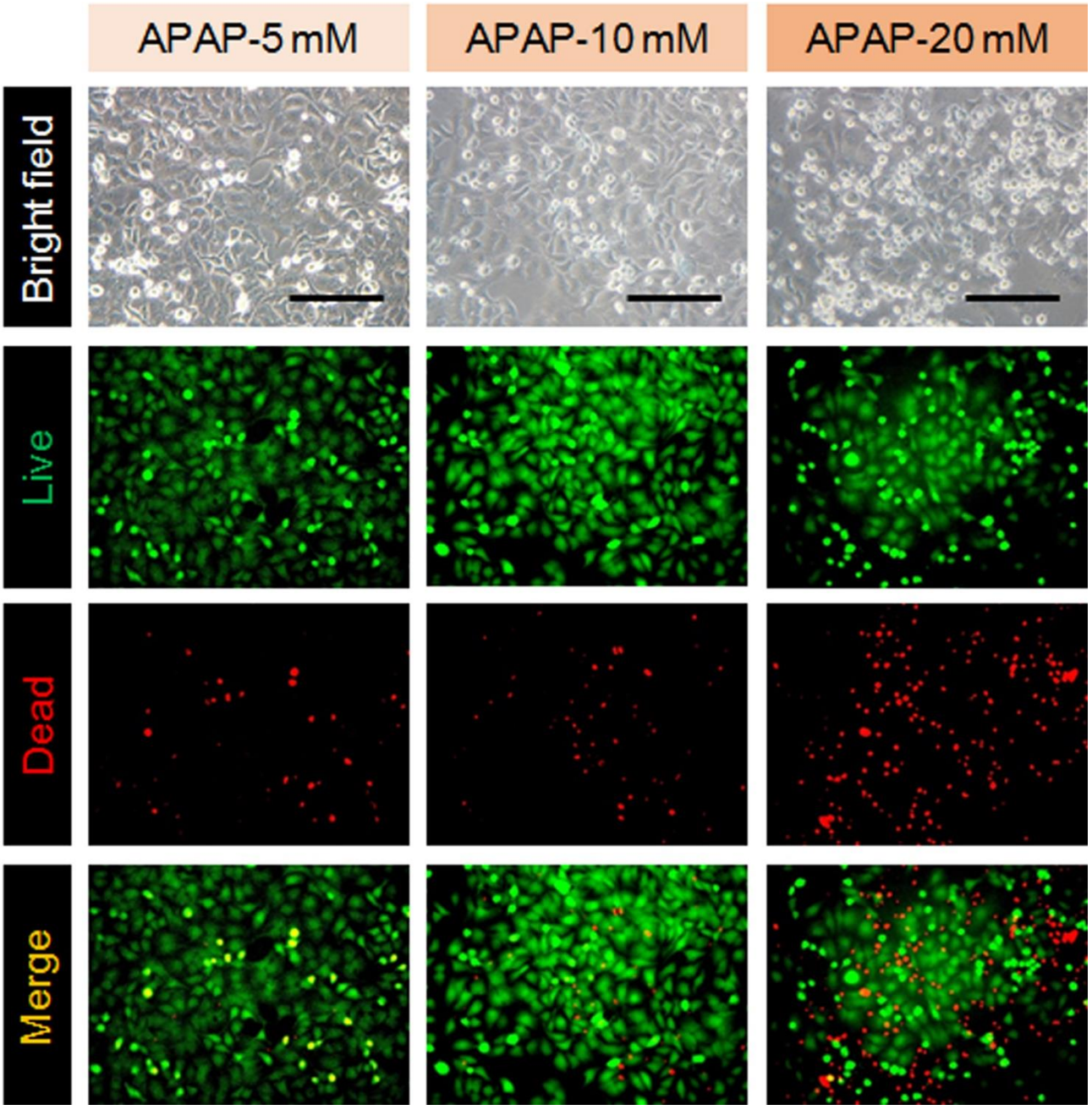

Figure S14. A set of bright-field images (the first row) and the corresponding FDA/PI co-staining fluorescent images (from the second to the fourth row: live, dead and merge) of HepG2 cells in Hep-2D culture model after treatment with three different concentrations of APAP for 24h. Live cells were stained green, and dead cells were stained red. Scale bar, 200 μm.

Supplementary Figure S15.

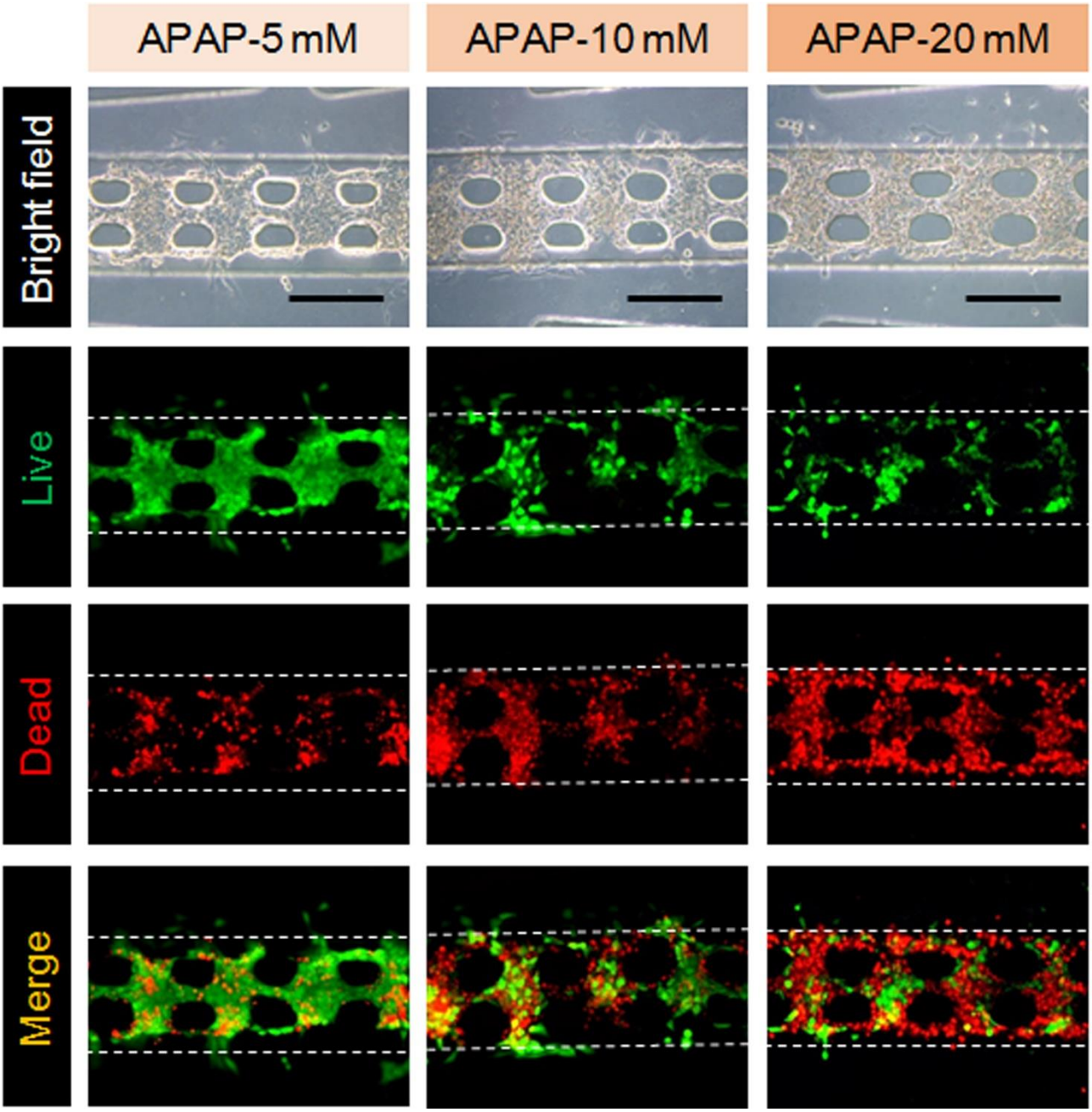

Figure S15. A set of bright-field images (the first row) and the corresponding FDA/PI co-staining fluorescent images (from the second to the fourth row: live, dead and merge) of HepG2 cells in Hep-3D culture model after treatment with three different concentrations of APAP for 24 h. Live cells were stained green, and dead cells were stained red. Scale bar, 200 μm.

Supplementary Figure S16.

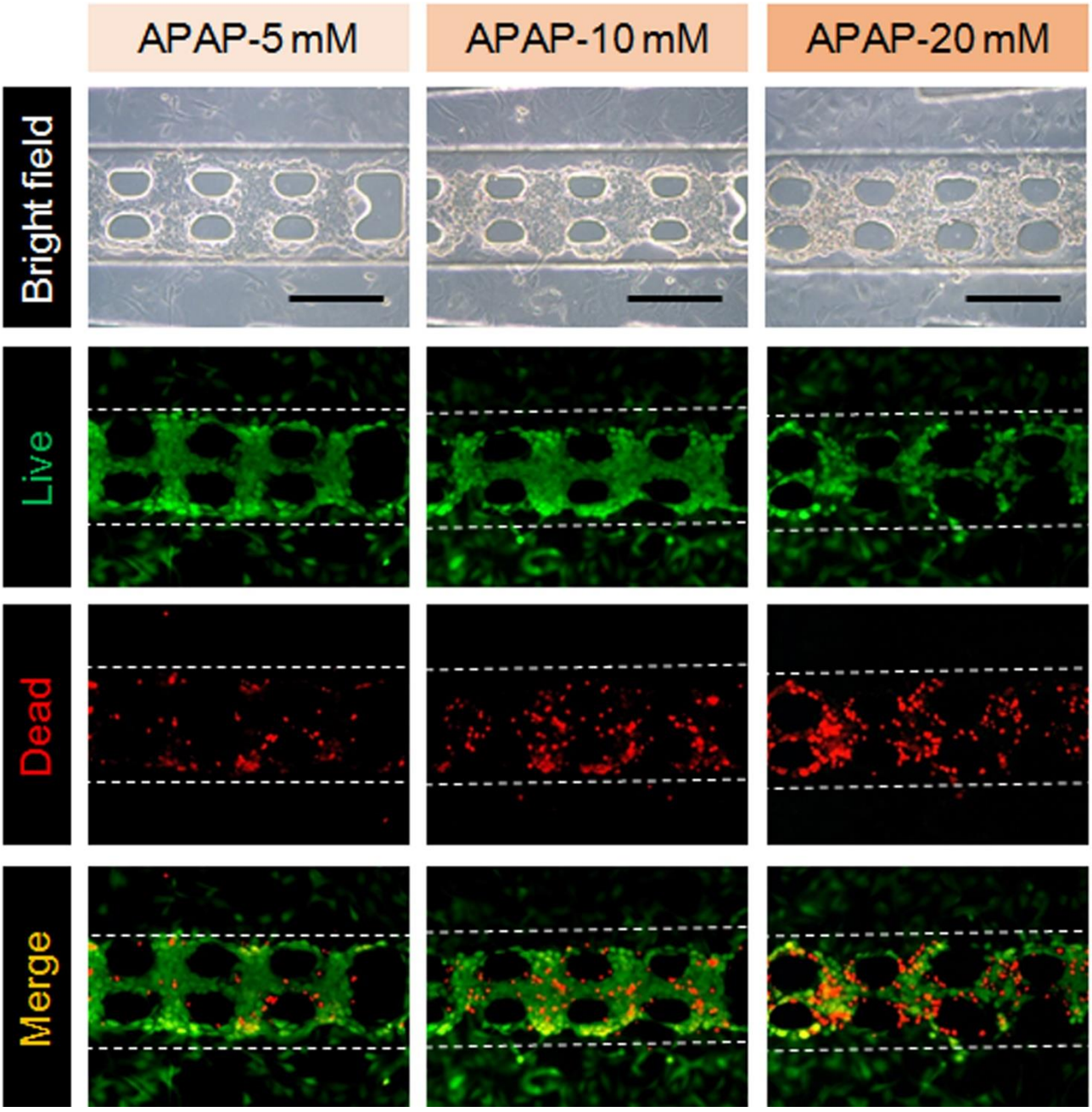

Figure S16. A set of bright-field images (the first row) and the corresponding FDA/PI co-staining fluorescent images (from the second to the fourth row: live, dead and merge) of HepG2 cells in liver lobule-like micro-tissue culture model after treatment with three different concentrations of APAP for 24 h. Live cells were stained green, and dead cells were stained red. Scale bar, 200 μm.

Supplementary Figure S17.

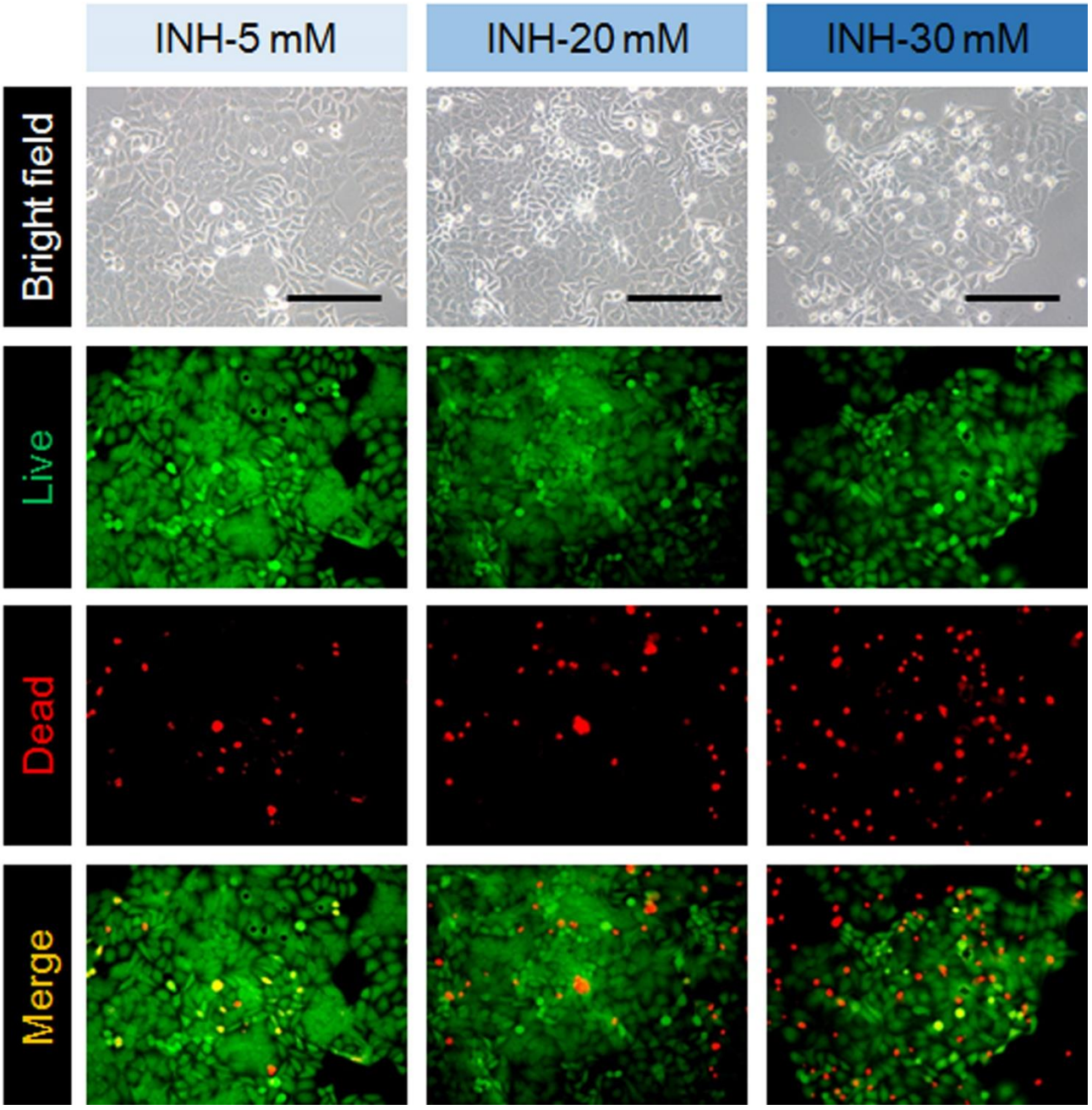

Figure S17. A set of bright-field images (the first row) and the corresponding FDA/PI co-staining fluorescent images (from the second to the fourth row: live, dead and merge) of HepG2 cells in Hep-2D culture model after treatment with three different concentrations of INH for 24 h. Live cells were stained green, and dead cells were stained red. Scale bar, 200 μm.

Supplementary Figure S18.

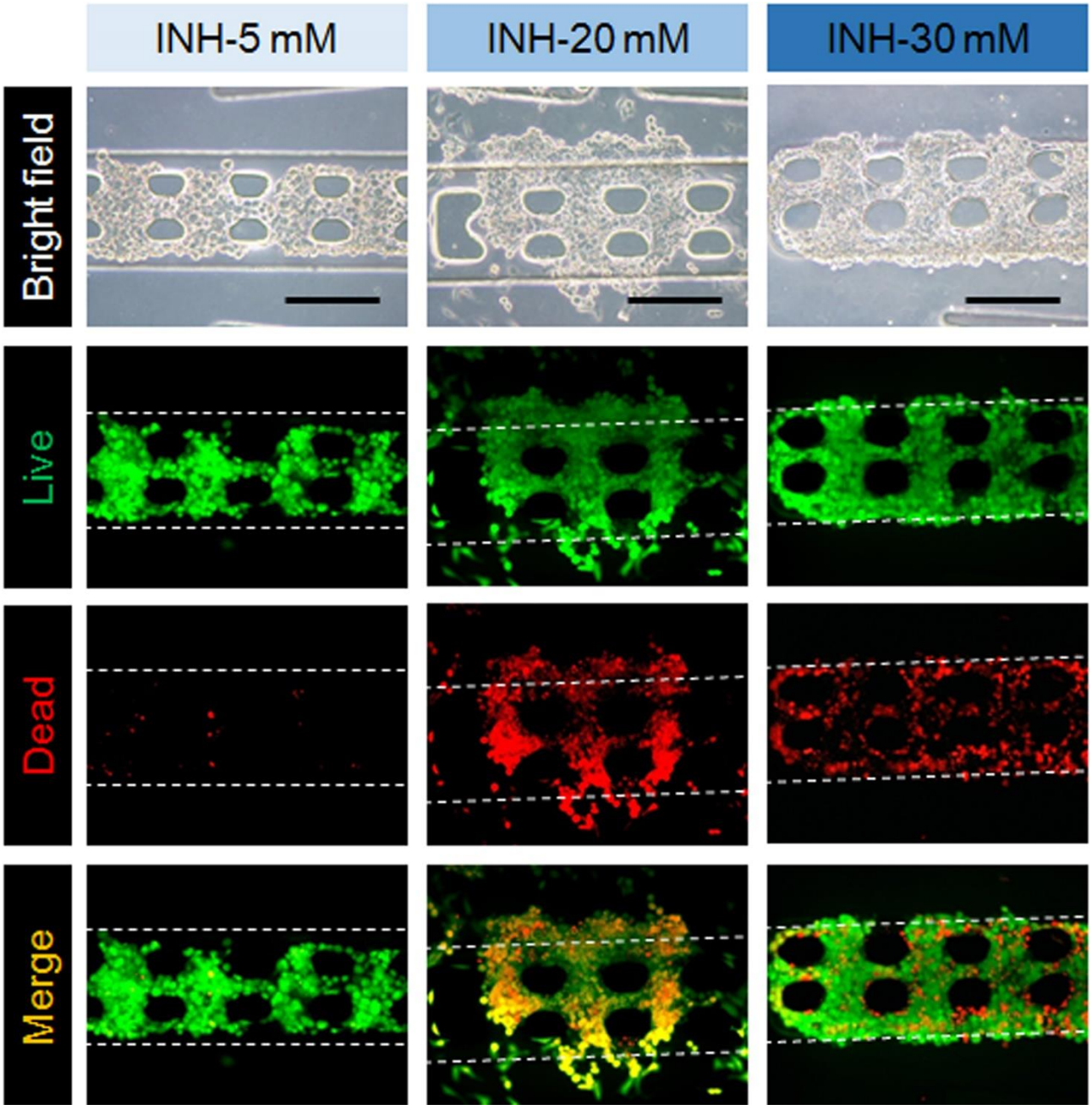

Figure S18. A set of bright-field images (the first row) and the corresponding FDA/PI co-staining fluorescent images (from the second to the fourth row: live, dead and merge) of HepG2 cells in Hep-3D culture model after treatment with three different concentrations of INH for 24h. Live cells were stained green, and dead cells were stained red. Scale bar, 200 μm.

Supplementary Figure S19.

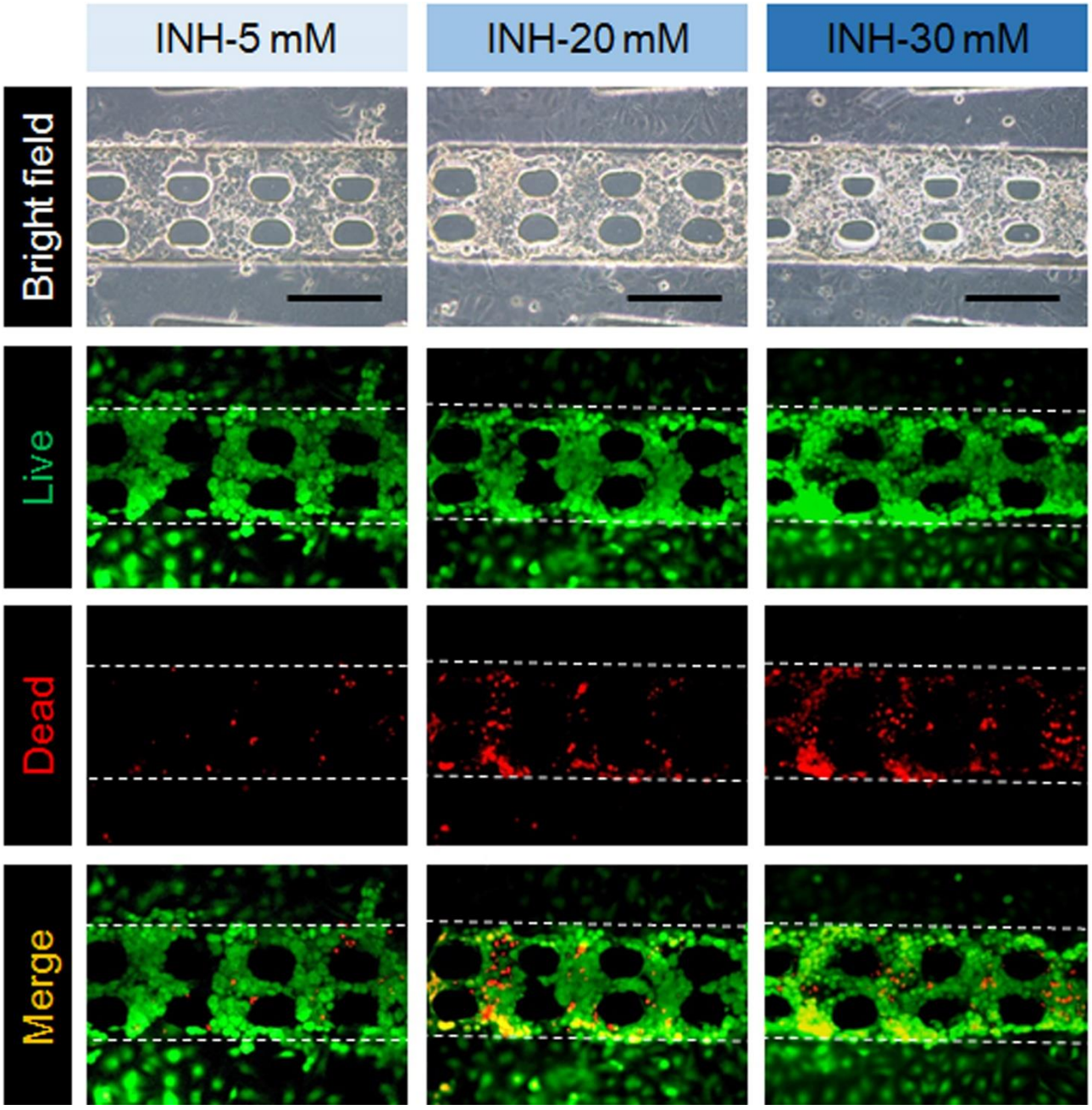

Figure S19. A set of bright-field images (the first row) and the corresponding FDA/PI co-staining fluorescent images (from the second to the fourth row: live, dead and merge) of HepG2 cells in liver lobule-like micro-tissue culture model after treatment with three different concentrations of INH for 24h. Live cells were stained green, and dead cells were stained red. Scale bar, 200 μm.

Supplementary Figure S20.

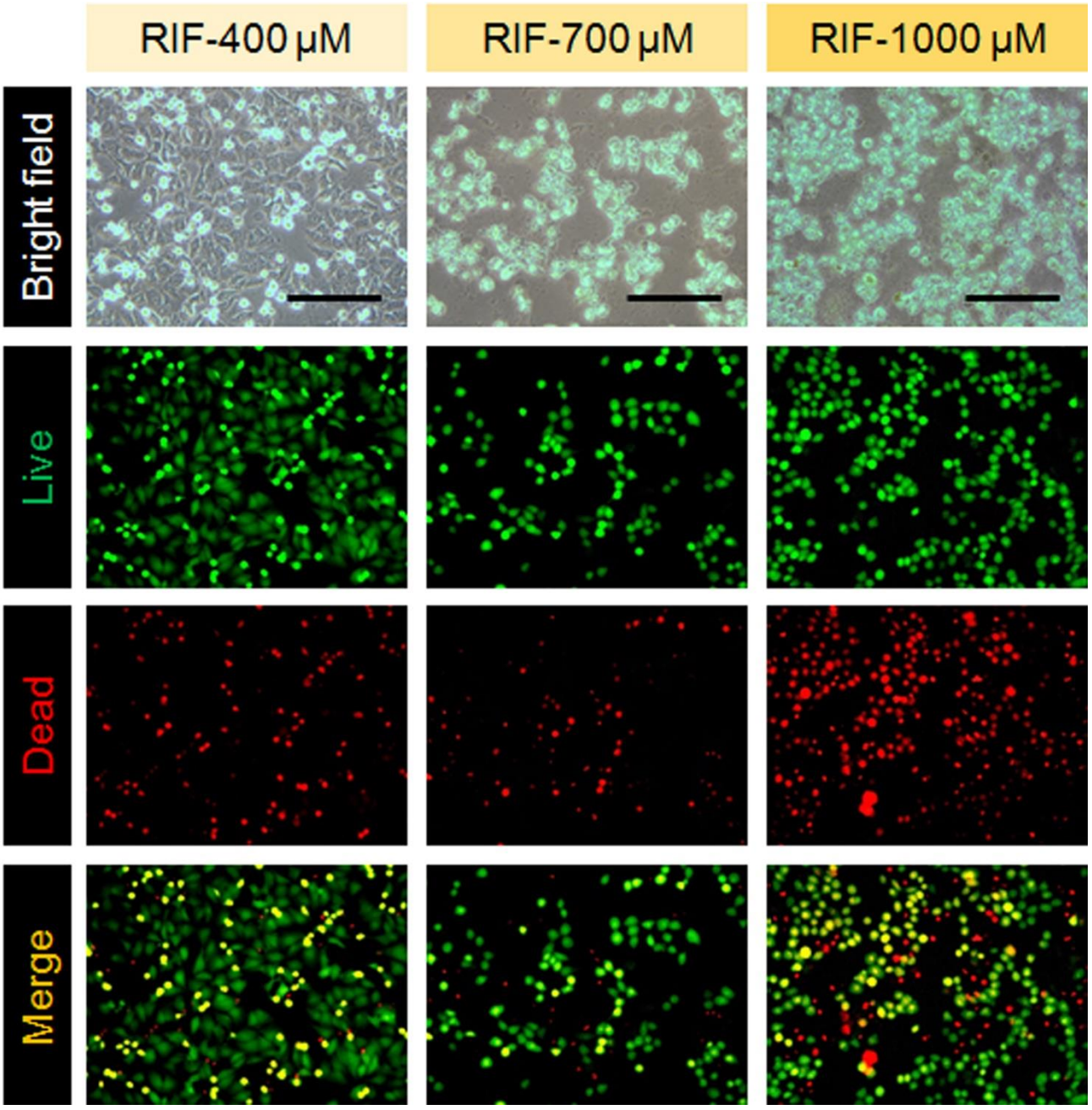

Figure S20. A set of bright-field images (the first row) and the corresponding FDA/PI co-staining fluorescent images (from the second to the fourth row: live, dead and merge) of HepG2 cells in Hep-2D culture model after treatment with three different concentrations of RIF for 24h. Live cells were stained green, and dead cells were stained red. Scale bar, 200 μm.

Supplementary Figure S21.

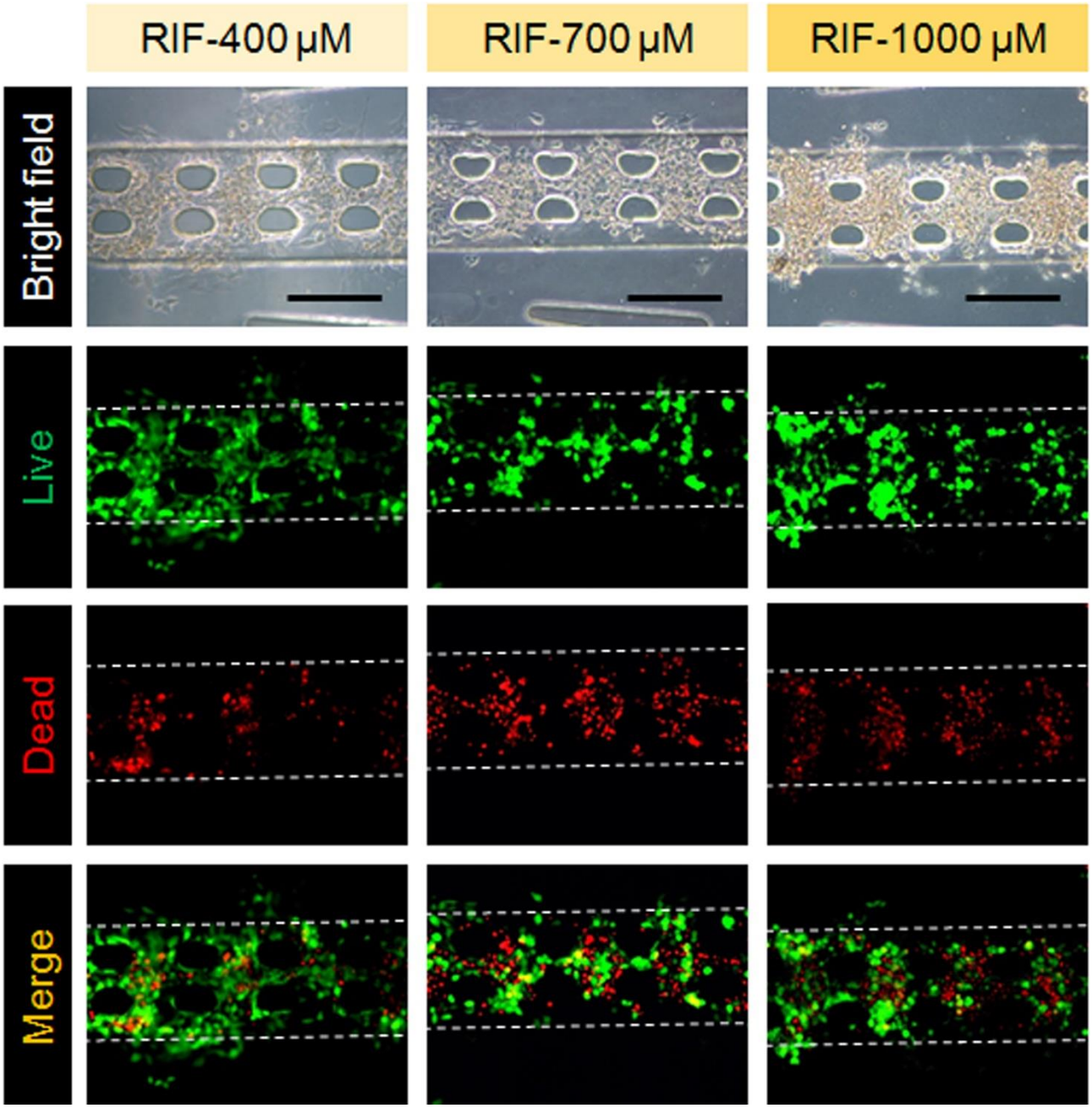

Figure S21. A set of bright-field images (the first row) and the corresponding FDA/PI co-staining fluorescent images (from the second to the fourth row: live, dead and merge) of HepG2 cells in Hep-3D culture model after treatment with three different concentrations of RIF for 24h. Live cells were stained green, and dead cells were stained red. Scale bar, 200 μm.

Supplementary Figure S22.

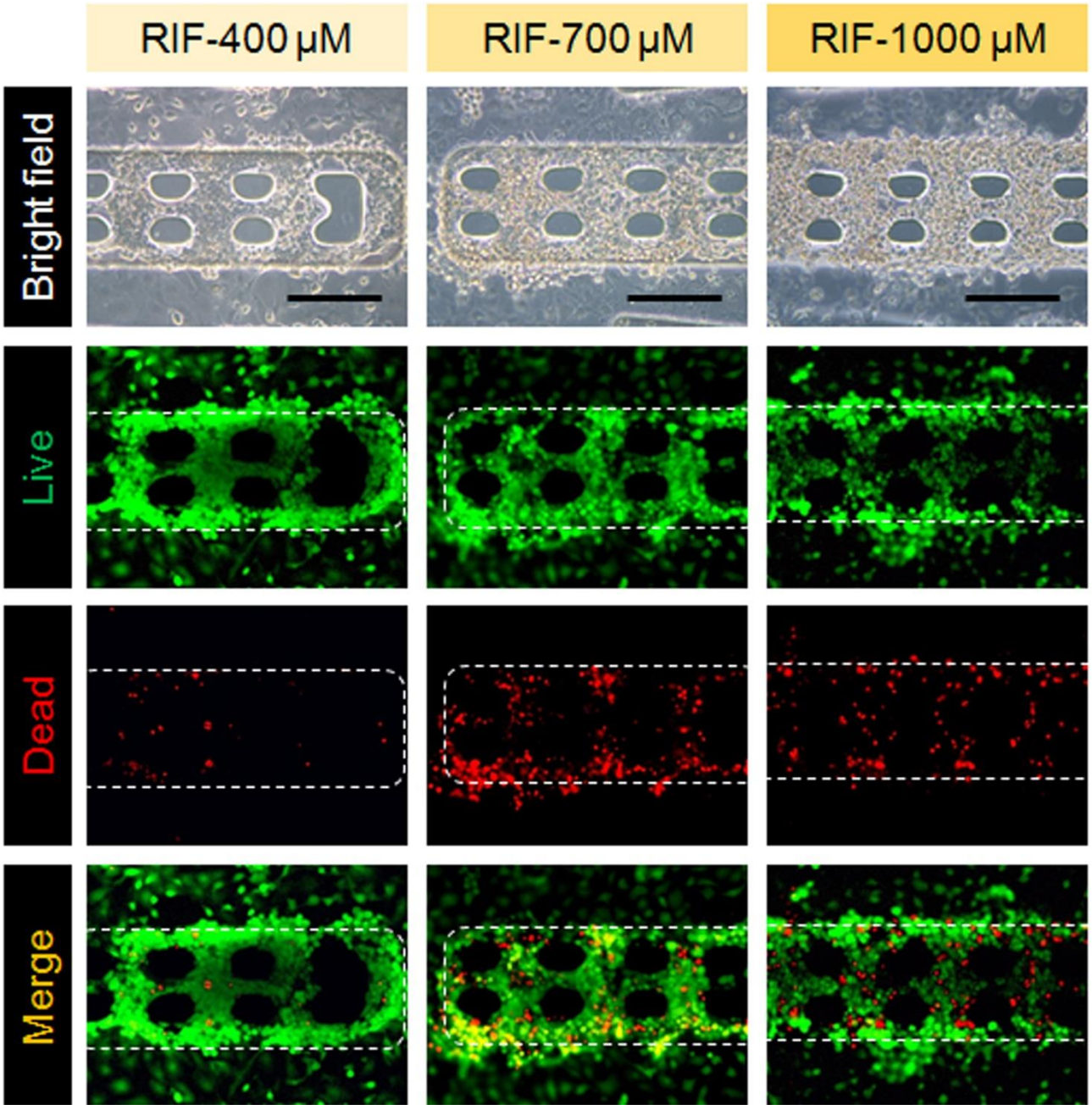

Figure S22. A set of bright-field images (the first row) and the corresponding FDA/PI co-staining fluorescent images (from the second to the fourth row: live, dead and merge) of HepG2 cells in liver lobule-like micro-tissue culture model after treatment with three different concentrations of RIF for 24h. Live cells were stained green, and dead cells were stained red. Scale bar, 200 μm.

Supplementary Figure S23.

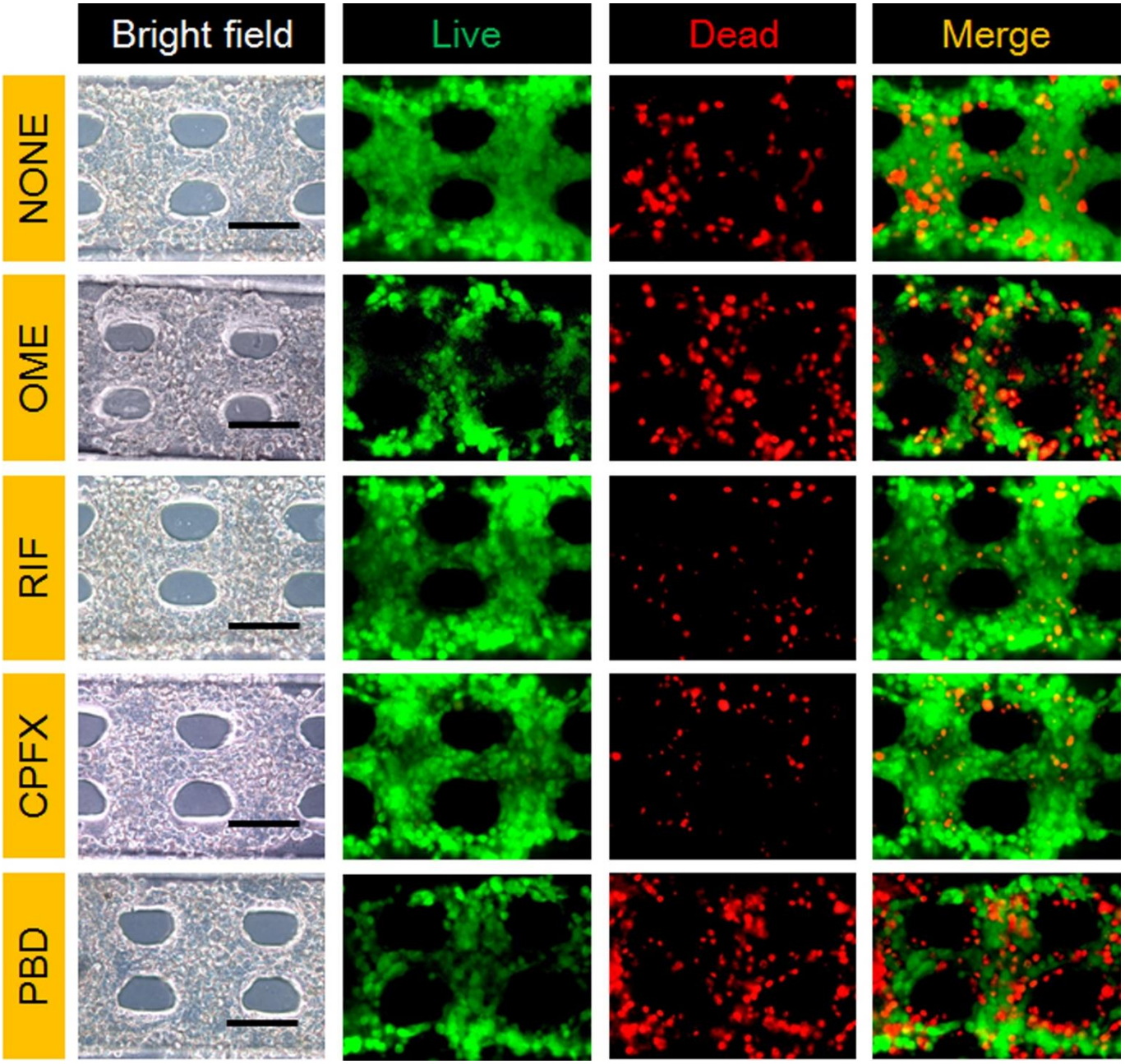

Figure S23. Detection of drug-drug interactions *via* the 3D biomimetic liver lobule-like micro-tissue. The micro-tissues were first normally cultured (non-treated, **NONE**, the first row) or exposed to pre-administrated drugs (i.e., omeprazole, **OME**, the second row; rifampicin, **RIF**, the third row; ciprofloxacin, **CPFX**, the fourth row; and probenecid, **PBD**, the fifth row) for 48 h, and then concurrently treated with APAP for 24 h. The viability of HepG2 cells was quantitatively measured with a FDA/PI co-staining method, by which live cells were stained green, and dead cells were stained red. A

set of bright-field images and the corresponding fluorescent images of HepG2 cells were timely recorded. The results showed that pre-incubation of the biomimetic micro-tissues with these drugs (i.e., OME, RIF, CPFX, and PBD) could agitate APAP-induced hepatotoxicity, indicating occurrence of drug-drug interactions. Scale bar, 100 μm.

Movie Captions

Movie S1. Micro-patterned immobilization of HepG2 cells with the actuated inner valve of PμS in a microfluidic device.

Movie S2. Site specific-inoculation of HAECs with the actuated PμS in a microfluidic device.

References for Supporting Information

(S1) He, J.; Ma, C.; Liu, W. M.; Wang, J. *Analyst* **2014**, *139*, 4482-4490.

(S2) Toh, Y. C.; Zhang, C.; Zhang, J.; Khong, Y. M.; Chang, S.; Samper, V. D.; van Noort, D.; Hutmacher, D. W.; Yu, H. *Lab Chip* **2007**, *7*, 302-309.

(S3) Thorsen, T.; Maerkl, S. J.; Quake, S. R. *Science* **2002**, *298*, 580-584.

(S4) Li, L.; Ren, L.; Liu, W. M.; Wang, J.-C.; Wang, Y.; Tu, Q.; Xu, J.; Liu, R.; Zhang, Y.; Yuan, M. S.; Li, T.; Wang, J. *Anal. Chem.* **2012**, *84*, 6444-6453.

(S5) Liu, W. M.; Wang, J.-C.; Wang, J. *Lab Chip* **2015**, *15*, 1195-1204.

(S6) Ho, C. T.; Lin, R. Z.; Chen, R. J.; Chin, C. K.; Gong, S. E.; Chang, H. Y.; Peng, H. L.; Hsu, L.; Yew, T. R.; Chang, S. F.; Liu, C. H. *Lab Chip* **2013**, *13*, 3578-3587.

(S7) Khetani, S. R.; Bhatia, S. N. *Nat. Biotechnol.* **2008**, *26*, 120-126.

(S8) Li, C. Y.; Stevens, K. R.; Schwartz, R. E.; Alejandro, B. S.; Huang, J. H.; Bhatia, S. N. *Tissue Eng. Part A* **2014**, *20*, 2200-2212.

(S9) Schwartz, R. E.; Fleming, H. E.; Khetani, S. R.; Bhatia, S. N. *Biotechnol. Adv.* **2014**, *32*, 504-513.